

# Magnetism and electronic structure calculation of SmN

C. Morari<sup>1</sup>, F. Beiușeanu<sup>2</sup>, I. Di Marco<sup>3</sup>, L. Peters<sup>4</sup>, E. Burzo<sup>5</sup>,  
S Mican<sup>5</sup>, and L. Chioncel<sup>6,7</sup>

<sup>1</sup> National Institute for Research and Development of Isotopic and Molecular Technologies, 65-103 Donath, RO-400293 Cluj Napoca, Romania

<sup>2</sup> Faculty of Science, University of Oradea, RO-410087 Oradea, Romania

<sup>3</sup> Department of Physics and Astronomy, Division of Materials Theory, Uppsala University, Box 516, SE-75120 Uppsala, Sweden

<sup>4</sup> Institute for Molecules and Materials, Radboud University Nijmegen, NL-6525 AJ Nijmegen, The Netherlands

<sup>5</sup> Babeș-Bolyai University Cluj-Napoca, RO-400084 Cluj-Napoca, Romania

<sup>6</sup> Augsburg Center for Innovative Technologies, University of Augsburg, D-86135 Augsburg, Germany

<sup>7</sup> Theoretical Physics III, Center for Electronic Correlations and Magnetism, Institute of Physics, University of Augsburg, D-86135 Augsburg, Germany

E-mail: liviu.chioncel@physik.uni-augsburg.de

**Abstract.** The results of the electronic structure calculations performed on SmN by using the LDA+U method with and without including the spin-orbit coupling are presented. Within the LDA+U approach, a N( $2p$ ) band polarization of  $\simeq 0.3 \mu_B$  is induced by Sm( $4f$ )-N( $2p$ ) hybridization, and a half-metallic ground state is obtained. By including spin-orbit coupling the magnetic structure was shown to be antiferromagnetic of type II, with Sm spin and orbital moments nearly cancelling. This results into a semiconducting ground state, which is in agreement with experimental results.

PACS numbers: 71.15.Ap;71.10.-w;73.21.Ac;75.50.Cc

## 1. Introduction

Rare-earth nitrides (RN) show a wide range of physical properties, despite having the same crystal structure with very close lattice constants and similar electronic structures. The structural, magnetic and electronic properties of rare-earth mononitrides were reviewed recently [1, 2]. In these reviews it was emphasized that the experimental data on the rare-earth mononitrides are rather scattered, and often lead to contradicting results, due to difficulties in obtaining samples of good quality. Thus, controversies concerning their electronic structure, transport and magnetic properties exist in literature. In the same reviews [1, 2] the results of different electronic structure calculations of RN compounds were also compared. The description of the strongly correlated  $4f$  states within the band theory is shown to require methods which go beyond density functional theory (DFT) in the standard local spin density approximation (LSDA). Band structure calculations were performed on the entire RN series using the self-interaction correction (SIC) method [3, 4, 5], and the LSDA+U method [6, 7]. For the latter, considering U corrections for  $4f$  bands only was shown to lead to a half-metallic ground state [7, 8]. If also the  $5d$  states are corrected with a local U term, the electronic structure of some RN turns out to be semiconducting, as shown for example for GdN [7].

SmN was reported to be an antiferromagnet having the Néel temperature  $T_N$  of 13 K [9] or 15 K [10]. From specific heat measurements an ordering temperature  $T_N$  of 18.2 K was reported [11]. No evidence of magnetic order was shown for  $T \geq 1.6$  K by neutron diffraction experiments [12]. A magnetic transition around 27 K was reported recently by Preston *et al.* [13]. The rather wide range of the reported ordering temperatures can be correlated with the compositions of the samples. The nitrogen vacancy lowers the Néel temperature, as in the case of GdN [14]. It was argued that SmN is likely to be in fact a metamagnet, however even in an applied field of  $\mu_0 H = 6$  T, the low temperature moment was smaller than  $0.1 \mu_B$ . The transport properties were also studied. A semimetallic behaviour of SmN was initially reported [15]. Later on, SmN was shown to be a semiconductor with a band gap of 0.7 eV [16]. Preston *et al.* [13] confirmed experimentally that in the studied temperature range ( $T \leq 150$  K) SmN shows a semiconducting behaviour.

Here we report the electronic and magnetic structure of SmN by using an LDA+U+SO approach. Several self-consistent solutions for different values of the parameter U exist in both ferro and anti-ferromagnetic configurations of the samarium moments. We discuss the energy difference between these self-consistent solutions and show that the ground state structure is that of an AF of type II according to Smart's classification [17] with vanishing moments and semiconducting in agreement with experimental results. In our calculations we have used several implementations. The most of our results have been obtained with the tight-binding linear muffin-tin orbitals (LMTO) method, in the atomic sphere approximation (ASA), by means of the code LMTO47 [18]. For sake of completeness we performed several calculations by means of

the full-potential (FP) LMTO code RSPt [19, 20, 21] and by means of the FP linearized augmented plane wave (LAPW) code FLEUR [22]. All these implementations include the on-site Coulomb interaction at the level of LSDA+U [23]. The +U contribution on the top of the LSDA represents the additional intra-atomic Hubbard repulsion among the localized electrons, treated self-consistently in a mean-field (“Hartree-Fock”) way. Used under appropriate conditions this contribution produces the correct insulating ground state for several systems where the standard LSDA band theory fails. All implementations used here consider the most general form of LSDA+U, where the interaction vertex is parametrized with a full spin and orbital rotationally invariant 4-index U-matrix [23, 24]. The addition of a Hubbard U interaction term in the energy functional, also introduces the need for a “double-counting” correction. The latter accounts for the fact that the Coulomb energy is already included (although not correctly) in the LSDA functional. The double-counting scheme is unfortunately not uniquely defined, and usually creates some ambiguity in the LSDA+U method [25, 26]. Here we adopt the so-called fully localized limit (FLL) double counting [23, 25, 27] which is suitable for strongly localized 4f electrons. It is crucial for the present study to consider the corrections due to the spin-orbit (SO) coupling self-consistently. We refer to these calculations in the followings with the acronym LSDA+U+SO [28]. More details on the construction of the local orbitals to supplement with the Hubbard U term can be found in the references above. Concerning the strenght of U, instead, we note that a direct evaluation of the average Coulomb and exchange integrals in terms of Clebsch-Gordan coefficients and Slater integrals usually produces unrealistically large values. For this reason Larson *et al.* in Ref. [7] scaled the values of the Slater-Coulomb integrals so that they fit the positions of the 4f-orbitals in Gd pnictides. The same semi-empirical screening has been applied to SmN, and produced the values  $U= 8.22$  eV and  $J= 1.07$  eV. Given that their study represents the most thorough and systematic computational work on the RN up to now, for sake of comparison we have used the same values.

This study is organized in three main parts. In the next section we present the results of LDA+U simulations by means of the ASA LMTO47 code. Then, the same code is employed to analyze the role of the spin-orbit coupling. In the last section results from the FP codes are presented, and used as term of comparison for the ASA results. A brief section summarizing the main conclusions of our study closes this manuscript.

## 2. LSDA+U calculations

The investigated SmN has the NaCl-structure, with the space group  $Fm\bar{3}m$  (no. 225) in which Sm occupies the (0, 0, 0) position and N is situated in  $(1/2, 1/2, 1/2)$ . The computational setup in ASA codes like LMTO47 involves a minimal set of basis functions for each atom in the unit cell. The radii of the muffin-tin spheres of Sm and N were set to 3.21 a.u. and 2.26 a.u. respectively. As usual for addressing non-close-packed lattices with ASA codes, empty spheres are needed. For SmN two empty spheres were

introduced in the  $(1/4, 1/4, 1/4)$  and  $(3/4, 3/4, 3/4)$  positions. The full Brillouin zone was sampled with a Monkhorst-Pack grid of  $(14 \ 14 \ 14)$   $\mathbf{k}$ -points. Considering the full Brillouin zone instead of the irreducible wedge is necessary to identify all possible local minima in LSDA+U, as discussed below. Finally the calculations were performed at the experimental lattice constant, i.e.  $a = 5.04 \text{ \AA}$ , and convergence was considered up to  $\mu\text{Ry}$ .

The resulting density of states is shown in Figure 1. The majority spin channel is metallic, while a gap of about 1.04 eV can be seen in the minority spin channel. The  $f$ -states are formed within the majority spin channel in the vicinity of the Fermi level, and at the same time a clear Sm( $f$ )-N( $p$ ) hybridization can also be seen. The Sm( $f$ )-N( $p$ ) hybridization is less pronounced in the minority spin channel. This result is consistent with the electronic structure calculation of Svane *et al.* [30] that demonstrates the presence of  $f$ -bands at the Fermi level, if the symmetry of the Sm( $4f$ ) density matrix is not broken artificially. In this case the three states transforming according to one of the three dimensional representations of the Oh group are partially occupied. If the cubic symmetry is broken, instead, one can access an insulating solution where one of these states is filled, while the other two states are empty [7]. This solution will be discussed in the next section, due to that it is the solution obtained when SO coupling is included.

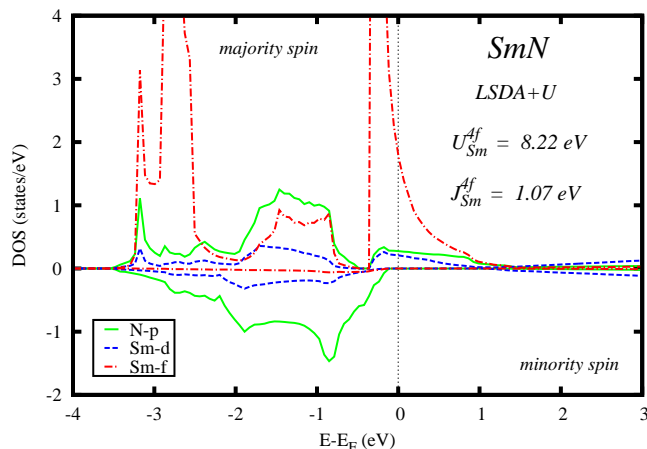


**Figure 1.** LSDA+U orbital resolved density of states of half-metallic SmN. The minority spin channel shows a gap of 1.04 eV. Minority spin Sm( $4f$ ) states are situated at higher energies (outside the plot range).

The N( $2p$ ) states are seen to dominate the top of the valence band in the minority spin channel. Analysing the band-structure plots (not shown) one notices that the N( $2p$ ) states are separated at the X symmetry point by a gap from the Sm( $5d$ ) states which are the dominant character of the bottom of the minority spin conduction band. For the majority electrons, where a metallic character is evidenced, a strong mixing between Sm( $4f$ ) and Sm( $5d$ ) states and N( $2p$ ) states takes place.

We note that the X-ray absorption and emission measurements of RN compounds are, in general, in good agreement with the density of states obtained from LSDA+U calculations, as emphasized in Ref. [2]. For SmN, however, our calculations, and also

those of Ref. [7] (with and without broken cubic symmetry), predict a zero gap in the majority spin band. Furthermore, there is evidence of some spectral weight at the bottom of the XES spectra, which was associated with the hybridization between N( $2p$ ) states and the highest occupied Sm( $4f$ ) states in agreement with LSDA+U band structure calculations. We should also mention that X-ray circular dichroism (XMCD) measurements clearly demonstrated that the N( $2p$ ) states are magnetically polarized in GdN, so we could expect that the polarization of N( $2p$ ) is also present in the SmN compound [31]. This is in fact clearly shown in the results of Figure 1.

Concerning the magnetic properties, the Sm spin moment is  $5.35\mu_B$ , out of which about  $0.05\mu_B$  belongs to the Sm( $5d$ ) bands, while for N( $2p$ ) bands a value of  $-0.35\mu_B$  was determined. The total magnetic moment per unit cell gives the integer value of  $5.00\mu_B$ , according to the half-metallic band structure. Obviously, these values cannot be compared with experimental data, since magnetism in RN requires the inclusion of SO coupling. For the sole purpose of obtaining orbital moments one can resort to the scheme devised by Larson *et al.* [7], where one-additional iteration with SO coupling is run on top of a converged LSDA+U simulation without SO coupling. In the present study, however, we cannot follow the strategy of Larson *et al.* [7], since it has not sufficient precision to determine the ground state among several magnetic configurations. Instead, we will perform full simulations by means of LSDA+U+SO, as illustrated in the next section. Before presenting these results it is important to note that the Hubbard U correction on the localized  $4f$  states may lead to several solutions, characterised by a different configuration in the  $4f$  local density matrix. To determine the ground state it is important to allow for all (or at least as many as possible) these local minima and identify the global one, as done by Larson *et al.* [7] and more recently by Peters *et al.* [29].

### 3. LSDA+U calculations including spin-orbit coupling

Neutron diffraction experiments on SmN [12] point to very small magnetic moments of the order of experimental errors. As a result, these experiments are not conclusive in determining the ground state magnetic structure, and theoretical calculations become of great importance. In this study we have analyzed theoretically various types of magnetic structures in order to obtain information on the ground state. For the actual computation we considered the rhombohedral representation of the NaCl structure, which corresponds to a 4 atom unit cell. In this lattice Sm atoms occupy the positions Sm1(0,0,0) and Sm2 (1,1,1) and nitrogen atoms are situated at (1/2, 1/2, 1/2) and (-1/2, -1/2, -1/2) sites. For the simulations with SO coupling, we have performed calculations with and without empty spheres, and figured out that the latter do not influence the qualitative results presented in the following.

Also within the LSDA+U+SO calculations one may obtain several local minima. In the presence of the SO coupling the symmetry is lowered and the energy landscape of self-consistent solutions is enriched with respect to the number of LSDA+U solutions.

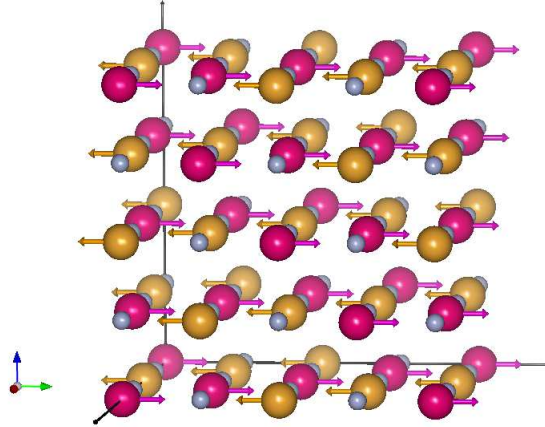


**Figure 2.** (color online) Model for the magnetic structure obtained by non-collinear LSDA+U+SO calculations. Large red/yellow circles (arrows) represent Sm1/Sm2 atoms (magnetic moments). Small gray circles represent the N atoms.

In the actual calculations, the initial conditions are translated into the different starting magnetic structures, i.e. the relative orientation of magnetization axes of the two Sm atoms in the unit cell. This is in fact possible as the LMTO47 code allows full non-collinear simulations. With this approach we have considered several ferromagnetic and antiferromagnetic orderings as starting configurations in which the magnetic moment of Sm1 atom situated in  $(0,0,0)$  was oriented either parallel or anti-parallel to the second samarium atom within the unit cell situated at Sm2 $(1,1,1)$ . Calculations have been performed with the direction of the moments along the Cartesian axis. In addition, other initial configurations with the moments direction along the diagonals of the cube have been also checked. Further on initial configurations with moments arranged within the  $(XY)$ ,  $(YZ)$ ,  $(ZX)$ , planes as well as out of plane configurations in a non-collinear setup have been considered. The self-consistent total energy calculations with SO coupling were performed for a Monkhorst-Pack grid of  $(24 \ 24 \ 24)$   $\mathbf{k}$ -points in the full Brillouin zone. The lowest total energy corresponding to the ground state magnetic configuration (among those studied) is presented in Figure 2, and is of type II antiferromagnetic. The energy difference between the ground-state and the ferromagnetic phase is of about 0.05 Ry for the selected values of  $U = 8.22$  eV. The type II antiferromagnetic ground state is very stable to variations of the strength of  $U$ , and was found to have the lowest energy also for values of  $U$  ranging from 6 to 10 eV.

The computed band structures for the selected values of  $U$  and  $J$  are presented in Figure 3. Both the parallel and anti-parallel arrangements of the samarium magnetic moments are presented, corresponding to the ferro and anti-ferromagnetic ordering. Both configurations exhibit gaps in the band structure. However, we must note that the Sm( $5d$ ) band falls below the Fermi energy at the F point for the parallel alignment (left panel of Figure 3), so this phase is in fact a semimetal, in agreement with Larson *et al.* [7]. For the ferromagnetic configuration the indirect gap is formed between the  $\Gamma$  point and  $\mathbf{k} = (-0.33 \ 0.00 \ 0.12)$ -point, and has a size of about 0.01 meV. In the anti-ferromagnetic

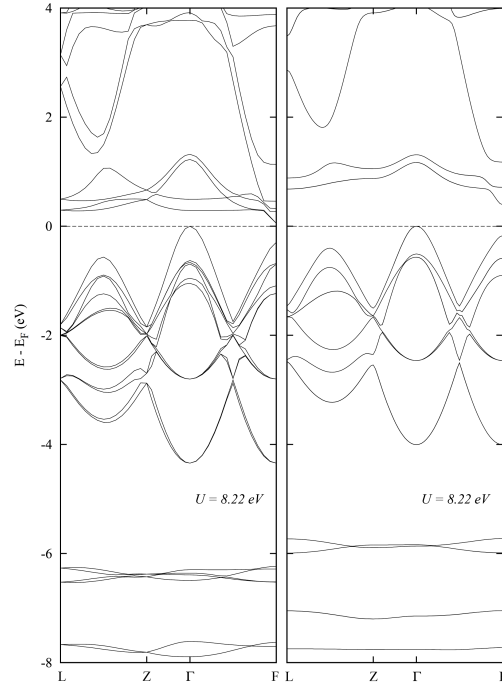


**Figure 3.** (color online) Computed band structures of SmN within the LSDA+U approach including spin-orbit coupling for the parallel (left panel) and anti-parallel (right panel) configurations.

configuration the gap is formed between the  $\Gamma$  point and the  $\mathbf{k} = (0.17 \ 0.29 \ 0.12)$ -point, and amounts to 0.40 meV. The size of the indirect gap is particularly significant, since it can be compared directly with experiment. Optical absorption measurements indicate the existence of a gap of about 0.7 eV [16]. We note that we can also simulate the non-groundstate anti-ferromagnetic configuration in the LSDA+U approach, without SO coupling. In this case we still obtain a semiconductor, but with a narrower gap of about 0.21 eV. Thus, including SO in a self-consistent way in addition to the LDA+U approach leads to the correct ground state and the right tendency of gap increasing. The magnitude obtained by calculations is still underestimated in comparison with the experimental values by a factor of two. An important role in the gap opening is played by the splitting of the  $4f$  manifold within LSDA+U+SO approach. In a cubic crystal field the  ${}^6H_{5/2}$  ground state splits into a  $\Gamma_7$  doublet and a  $\Gamma_8$  quartet. Specific heat measurements indicate that the doublet is lowest in energy. The rhombohedral representation used in the computations has a lower symmetry. This makes it possible to obtain the splitting described in the previous section without breaking the symmetry with ad-hoc corrections through the LSDA+U potential. Results show that the  $4f$  states are splitted. The empty  $4f$  bands occur about 1 eV above the Fermi energy, while the occupied  $4f$  states are positioned at around 6 eV below it, for  $U = 8.22$  eV. This splitting happens for both parallel and antiparallel alignment, as evident from Figure 3.

From our simulations we can extract the SO coupling constant  $\lambda \approx 0.16$  eV. This

value is significantly smaller than the exchange (Hund) interaction parameter  $J = 1.07$  eV, which demonstrates that for this compound a relatively weak SO interaction exists. This weak interaction results in a Russell-Saunders (LS coupling) scheme with the spin  $\mathbf{S}$  and the orbital  $\mathbf{L}$  operators being well defined. In such a case the LS-basis is formed by the eigenfunctions of both spin  $\mathbf{S}$  and orbital  $\mathbf{L}$  moment operators. For our parameters U and J, in the ferromagnetic configuration, we obtained a Sm(4*f*) contribution to the spin moment equal to  $\mathbf{S}^{Sm} = 5.00 \mu_B$ , while the orbital moment contribution is  $\mathbf{L}^{Sm} = -4.57 \mu_B$ . In the anti-parallel configuration, instead, we obtained a Sm(4*f*) contribution to the spin moment equal to  $\mathbf{S}^{Sm} = 4.99 \mu_B$ , while the orbital moment contribution is  $\mathbf{L}^{Sm} = -4.53 \mu_B$ . In both cases the spin and orbital moments are anti-parallel, i.e. they are arranged with respect to the third Hund's rule. The atomic-like behavior of these moments is also clear from their stability with respect to the magnetic configuration. From the computed values of  $|\mathbf{S}|$  and  $|\mathbf{L}|$  the Landé factor and the Sm(4*f*) magnetic moment were calculated, the obtained values being  $g = 0.18$  and  $\mu_{Smf} = 0.36 \mu_B$ .

It is interesting to analyze how these results change by varying the values of U and J. In fact, limiting our calculations to values extracted to match a few selected experimental properties is too much prone to an error, especially in light of the limitations that experiment have for RNs. We have therefore evaluated the magnetic properties for a higher value of U, i.e.  $U = 9.22$  eV. This corresponds to an increment of 1 eV with respect to our selected value. We obtained a SO coupling constant  $\lambda \approx 0.17$  eV. The magnetic moments due to the Sm(4*f*) states in the anti-parallel configurations became  $\mathbf{S}^{Sm} = 4.97 \mu_B$  and  $\mathbf{L}^{Sm} = -4.63 \mu_B$ . These values exhibit an expected increase of the orbital polarization, which is compensated by a slight decrease of the spin moment. The computed Landé factor and Sm(4*f*) magnetic moment were  $g = 0.21$  and  $\mu_{Smf} = 0.55 \mu_B$ . These values lead to the same physical picture outlined above.

Thus, we conclude that the magnetic structure of SmN is essentially of AF-type II. Such magnetic structures were shown in GdX [32] and TbX [16], with X = P, As, Sb and Bi. Although the spin and orbital moments of Sm nearly cancel, finite values of SmN magnetizations can be obtained. These can be correlated with the contributions of Sm(5*d*) and N(2*p*) band polarizations resulting mainly from the hybridization with the Sm(4*f*) band.

#### 4. Full potential calculations

Given that the structure of SmN is not strictly close-packed, we have checked our main results by means of the RSPt code [19, 20, 21], which is based on the FP-LMTO method. The calculations were limited to the AFM phase of SmN, and were performed with Sm(6*s*, 6*p*, 5*d*, 4*f*) and N(2*s*, 2*p*) orbitals for the valence electrons. The radii of the muffin-tin spheres of Sm and N were set to 2.5 a.u. and 2.0 a.u. respectively. The number of kinetic energy tails, describing the basis in the interstitial region between the muffin-tin spheres, was set to 3 for the *s* and *p* states, and to 2 for the *d* and *f*

states. These parameters have been carefully checked to offer a converged basis. The full Brillouin zone was sampled with a Monkhorst-Pack grid of (24 24 24)  $\mathbf{k}$ -points.

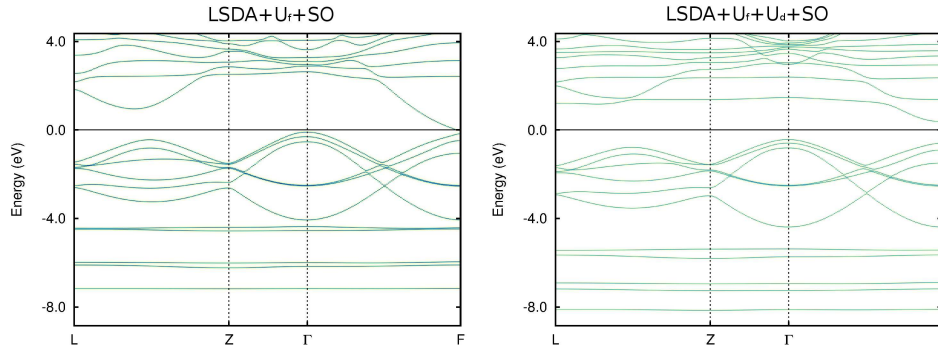


**Figure 4.** (color online) Computed band structures of SmN within the LSDA+U approach including spin-orbit coupling by means of the FP-LMTO code RSPt. Results without and with an additional Hubbard correction  $U_d$  are shown, respectively in the left panel and right panel.

We have analyzed the magnetic anisotropy in the AFM phase of type II. We have confirmed that the easy axis is aligned towards the y-direction, for both DFT in LDA with SO coupling and LSDA+U+SO. For the simulations where the magnetization is aligned along the easy axis, the values of the Sm(4*f*) contribution to the spin and orbital moment are  $\mathbf{S}^{Sm} = 4.09 \mu_B$  and  $\mathbf{L}^{Sm} = -3.46 \mu_B$ . Although to a first sight these values may look rather different than those presented in the previous section, we have to keep in mind that in a FP code the muffin-tin spheres cannot overlap, and an important contribution to the magnetic moments may lay in the interstitial region. In addition to the magnetic properties, we have also computed the electronic structure, which is reported in the left panel of Figure 4. Here one can see a major difference with respect to the data reported in Figure 3. In fact the electronic structure obtained in a FP code presents semi-metallic character, similarly to what observed above for the FM phase. The presence of states within the gap changes considerably the physical picture related to the band structure with respect to the LMTO47 simulations. To understand if this behavior is due to the ASA character or to more implementation specific details, we performed additional FP simulations with the LAPW code FLEUR [22]. Indeed, we obtained very similar band structures (not shown) as those reported in the left panel of Figure 4. The difference among ASA and FP calculations creates an important problem. On the one hand the FP simulations must be preferred for accuracy and reliability, on the other hand the experimental data seem to support the insulating solution obtained in ASA (see above). The problem of the absence of an energy gap has been discussed in detail by Larson *et al.* [7] for the ferromagnetic phase. There the authors suggest that an insulating character can be obtained by means of an additional Hubbard correction for the Sm(5*d*) states. They determine a  $U$  parameter equal to 6.4 eV in order to fix the experimental band gap of GdN, while  $J$  was set to zero for sake of simplicity. With these parameters they obtain a semi-metallic solution for the FM phase of SmN,

where the indirect band gap is of about -0.15 eV. We have followed their strategy, and performed LSDA+U+SO simulations of the AFM phase with this setup. The resulting band structure is reported in the right panel of Figure 4. A band gap is now opened, analogously to what reported in Figure 3. It is interesting to note how the Hubbard correction to the  $\text{Sm}(5d)$  states also changes the position (but not the relative splitting) of the  $\text{Sm}(4f)$  levels.

## 5. Conclusion

In the present paper we have discussed the magnetic and the electronic structure properties of the  $\text{SmN}$  compound. The sensitivity of the macroscopic properties to temperature, pressure and impurities is primarily due to the complex interplay between the rare-earth  $4f$ - $5d$  interactions and the hybridization between  $\text{Sm}(4f)$  states with the  $N(2p)$  states. The electronic structure results based on the LSDA+U method favor a half-metallic ground state, whereas if we include the spin-orbit coupling a magnetic AF-type II structure is obtained with moments that nearly cancel. The nearly linear field dependence of the  $\text{SmN}$  magnetization, at 2 K, experimentally observed in a thin film close to being stoichiometric, [13] is not in contradiction with AF ordering. In addition, the presence of SO coupling leads to an enlarged semiconducting gap. However, the magnitude of the gap is still underestimated, in comparison with the experimental measurements, an indication that the present LDA+U+SO calculations does not give a complete description. Full-potential calculations show, in fact, that the observed gap arises mainly due to the restrictions imposed by the atomic-sphere approximation and not because of the Coulomb interaction. A more physical description of the band gap can be obtained with an explicit Hubbard correction for the  $\text{Sm}(5d)$  states. However, this approach presents two important problems. First, it introduces another parameter in the simulations; second it is indeed hard to justify the presence of a local Hubbard term to improve the description of the highly delocalized  $5d$  states. In this context, ASA simulations have the advantage of giving a physically correct solution without needing additional semi-empirical corrections. Anyway, once the band gap is present, possible metal-semiconductor transitions are expected upon doping or upon changing external conditions. In such cases an important role is played by not only the aforementioned  $d$ - $d$  interaction, but also by the  $f$ - $d$  and  $f$ - $s$  hybridizations. These effects are finally entangled with the multiplet structure of the atomic-like  $4f$  states. In order to consider the multiplet structure properly, an approach beyond the static mean-field is needed. The LDA+DMFT approach [33, 34, 35] in the Hubbard I approximation [35, 36] is capable of capturing all these effects, and has already been applied to the paramagnetic ErAs [37], and to TbN [29]. This type of calculations introduce additional difficulties that we plan to address in our future research.

## Acknowledgments

The calculations were performed in the Datacenter of NIRDIMT. C Morari acknowledges the financial support offered by the Augsburg Center for Innovative Technologies (ACIT), University of Augsburg, Germany. S Mican would like to acknowledge support from project POSDRU/88/1.5/S/60185-“Innovative doctoral studies in a knowledge based society”. I Di Marco and L Peters acknowledge the Nederlandse Organisatie voor Wetenschappelijk Onderzoek (NWO), and the Swedish National Allocations Committee (SNIC/SNAC) for computational time at the National Supercomputer Cluster (NSC). Also SURFsara is acknowledged for the usage of LISA and their support.

## References

- [1] Duan C-G, Sabirianov R F, Mei W N, Dowben P A, Jaswal S S and Tsymba E Y 2007 *J. Phys.: Condens. Matter* **19** 315220
- [2] Natali F, Ruck B J, Plank N O V, Trodahl H J, Granville S, Meyer C and Lambrecht W R L 2013 *Progress in Materials Science* **58** 1316
- [3] Aerts C M, Strange P, Horne M, Temmerman W M, Szotek Z and Svane A 2004 *Phys. Rev. B* **69** 045115
- [4] Horne M, Strange P, Temmerman W M, Szotek Z, Svane A and Winter H 2004 *J. Phys.: Condens. Matter* **16** 5061–70
- [5] Szotek Z, Temmerman W M, Svane A, Petit L, Strange P, Stocks G M, Ködderitzsch D K, Hergert W and Winter H 2004 *J. Phys.: Condens. Matter* **16** S5587-S5600
- [6] Larson P and Lambrecht W R L 2006 *Phys. Rev. B* **74** 085108
- [7] Larson P, Lambrecht W R L, Chantis A and Van Schilfgaarde M 2007 *Phys. Rev. B* **75** 045114
- [8] Burzo E, Bucur N, Allmaier H and Chioncel L 2008 *J. Opt. Adv. Mat* **10** 389
- [9] Schumacher D P and Wallace W E 1966 *Inorg. Chem.* **5** 1563
- [10] Busch G, Junot P, Levy F, Menth A and Vogt O 1965 *Phys. Lett.* **14** 264
- [11] Stutius W 1969 *Phys. Kondens. Matt.* **10** 152
- [12] Moon R M and Koehler W C 1969 *J. Magn. Magn. Mater.* **14** 256
- [13] Preston A R H, Granville S, Housden D H, Ludbrook B, Ruck B J, Trodahl H J, Bittar A, Williams G V M, Downes J E and DeMasi A *et al* 2007 *Phys. Rev. B* **76** 245120
- [14] Cutler R A and Lawson A W 1975 *J. Appl. Phys.* **46** 2739
- [15] Didchenko D and Gortsema F P 1963 *J. Phys. Chem. Solids* **24** 863
- [16] Hullinger F 1979 *Handbook on the Physics and Chemistry of Rare Earths* vol 4 ed Gschneider K A and LeRoy E (Amsterdam: North-Holland) pp 153–256
- [17] Smart J S 1966 *Effective Field Theories of Magnetism* (Philadelphia: Sanders)
- [18] Andersen O K 1975 *Phys. Rev. B* **12** 3060–83
- [19] Wills J M, Alouani M, Andersson P, Delin A, Eriksson O and Grechnev O 2010 *Full-Potential Electronic Structure Method* in *Electronic Structure and Physical Properties of Solids: Springer Series in Solid-State Sciences* (Berlin: Springer-Verlag)
- [20] Di Marco I, Minár J, Chadov S, Katsnelson M I, Ebert H and Lichtenstein A I 2009 *Phys. Rev. B* **79** 115111
- [21] Grånäs O, Di Marco I, Thunström P, Nordström L, Eriksson O, Björkman T and Wills J M 2012 *Computational Materials Science* **55** 295
- [22] <http://www.fleur.de>
- [23] Anisimov V I, Aryasetiawan F and Lichtenstein A I 1997 *J. Phys.: Condens. Matter* **9** 767–808
- [24] Shick A B, Drchal V and Havela L 2005 *Europhys. Lett.* **69** 588
- [25] Petukhov A G, Mazin I I, Chioncel L and Lichtenstein A I 2003 *Phys. Rev. B* **67** 153106

- [26] Ylvisaker E R, Pickett W E and Koepernik K 2009 *Phys. Rev. B* **79** 035103
- [27] Liechtenstein A I, Anisimov V I and Zaanen J 1995 *Phys. Rev. B* **52** R5467
- [28] Shorikov A O, Lukoyanov A V, Korotin M A and Anisimov V I 2005 *Phys. Rev. B* **72** 024458
- [29] Peters L, Di Marco I, Thunström P, Katsnelson M I, Kirilyuk A and Eriksson O 2014 *Phys. Rev. B* **89**, 205109
- [30] Svane A, Kanchana V, Vaitheeswaran G, Santi G, Temmerman W M, Szotek Z, Strange P, and Petit L 2005 *Phys. Rev. B* **71** 045119
- [31] Leuenberger F, Parge A, Felsch W, Fauth K, and Hessler M 2005 *Phys. Rev. B* **72** 014427
- [32] Li D X, Haga Y, Shida H, Suzuki T, Kwon Y S and Kido G 1997 *J. Phys.: Condens. Matter* **9** 10777
- [33] Kotliar G, Savrasov S Y, Haule K, Oudovenko V S, Parcollet O, and Marianetti C A 2006 *Review Modern Physics* **78** 865
- [34] Held K 2007 *Advances in Physics* **56** 829
- [35] Lichtenstein A I, and Katsnelson M I 1998 *Phys. Rev. B* **57** 6884–95
- [36] Hubbard J 1963 *Proc. R. Soc. London* vol 276 p 238
- [37] Pourovskii L V, Delaney K T, Van de Walle C G, Spaldin N A and Georges A 2009 *Phys. Rev. Lett.* **102** 096401